CHAPTER IV
RESULTS AND DISCUSSION

4.1 PANI Synthesis

There are several ways to polymerize PANI but because of its poor solubility in water, PSS is introduced to provide a water solubility. Interfacial and bulk polymerization were used to synthesize PANI. For the interfacial polymerization, 2 phases used were water and chloroform. As shows on Figure 4.1, an aqueous phase contained H_2SO_4, APS and PSS while chloroform contained ANI monomer. H_2SO_4 was used to protonate ANI monomer at the interface then PSS came to pick up ANI monomer by an electrostatic interaction and π-π interaction between the benzene rings on PSS and ANI after that APS was used to initiate ANI to polymerize to PANI (Detsri *et al.*, 2013). For bulk polymerization, ANI and PSS were dissolved together with H_2SO_4 to bind ANI to PSS first then added APS to polymerize ANI to PANI (Yang *et al.*, 1997).

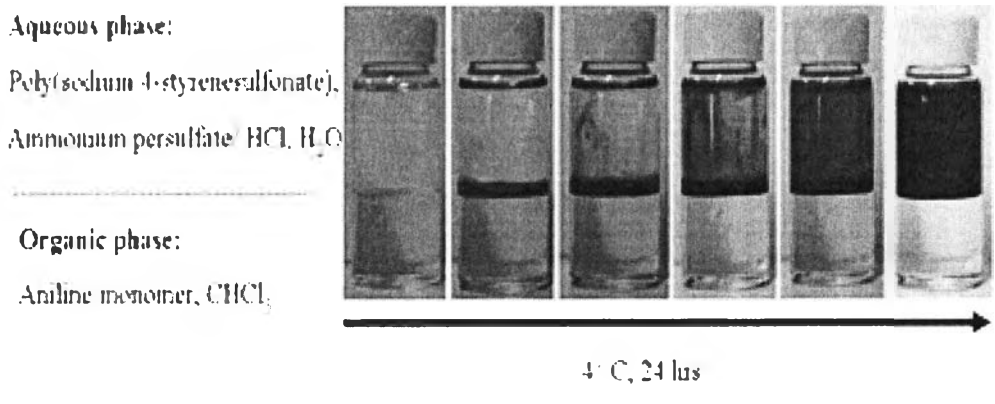

Figure 4.1 The interfacial synthesis of polyaniline with PSS as template.

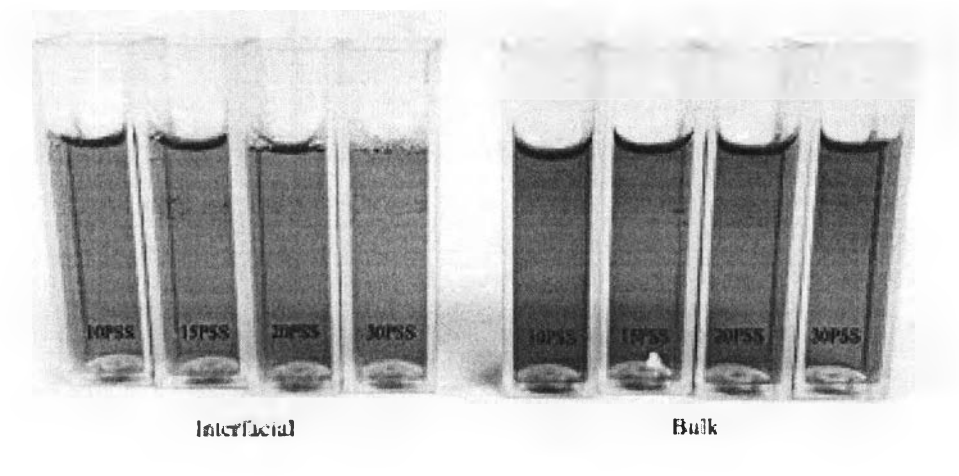

Figure 4.2 PANI-PSS solution after interfacial and bulk polymerization.

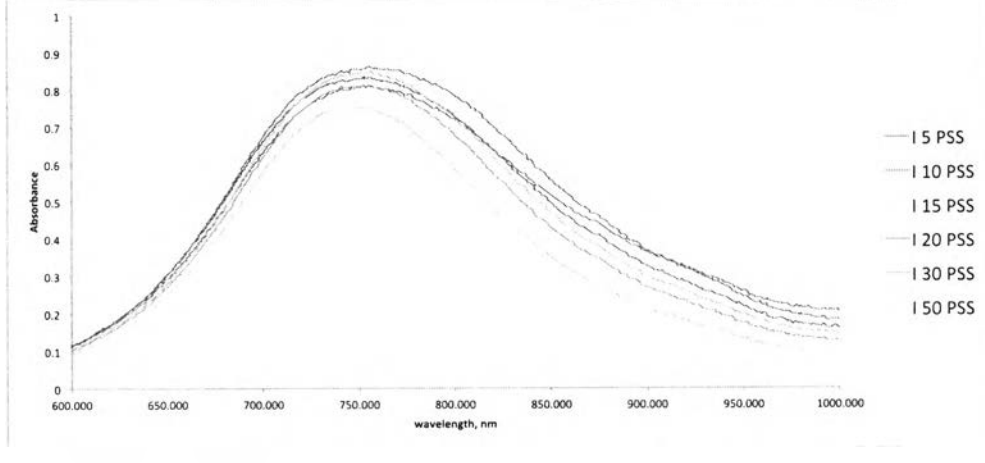

Figure 4.3 UV spectrum of aqueous phase after interfacial polymerization at different PSS concentration.

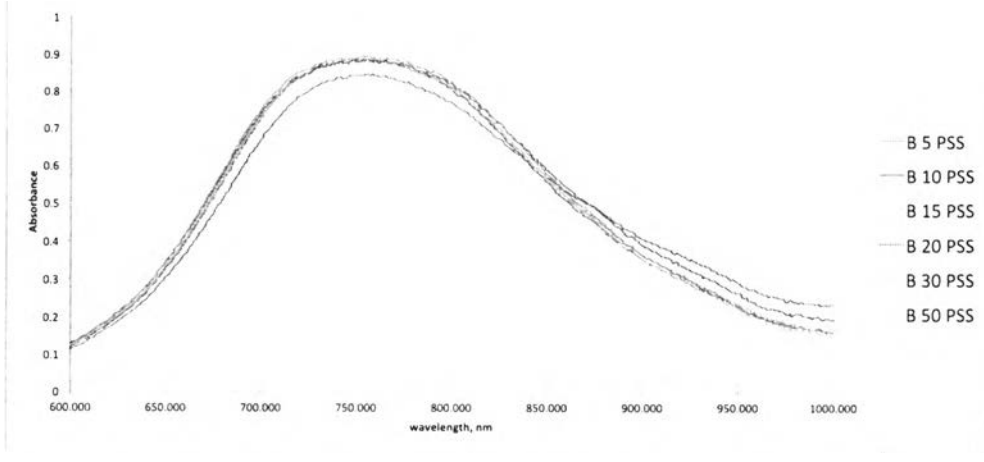

Figure 4.4 UV spectrum of aqueous phase after bulk polymerization at different PSS concentration.

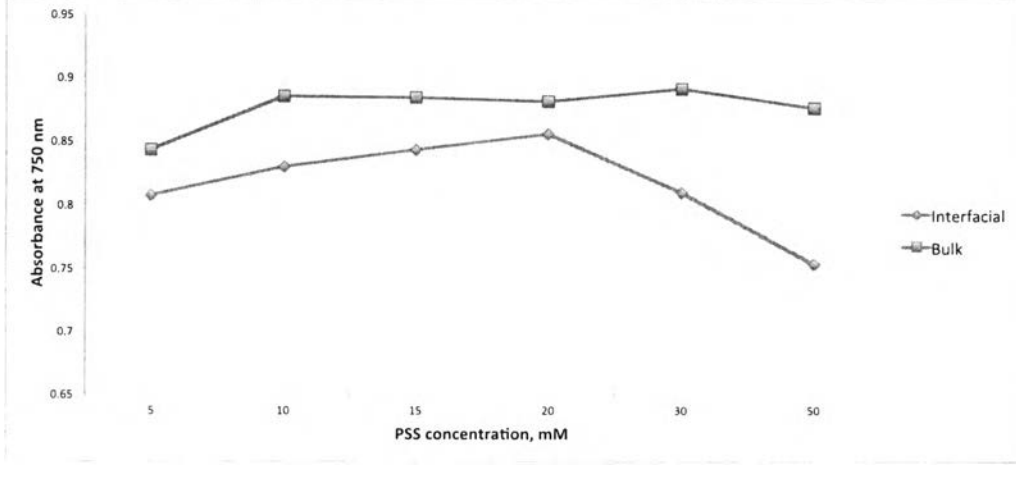

Figure 4.5 Change in absorbance of the aqueous phase after interfacial and bulk polymerization as a function of PSS concentration.

Yield of the reaction can be measured using UV-Vis spectrophotometer by looking at an absorbance at a wave length equal to 750 nm which was a characteristic of green PANI as shown on Figure 4.2, 4.3 and 4.4. Figure 4.5, it can be seen that bulk polymerization gave higher yield than an interfacial method because of the higher monomers in the solution that were polymerized. The effect of PSS

concentration that was used to stabilize PANI in water was studied. At 5 mM PSS in bulk polymerization, there was not enough PSS to provide a completed water solubility to PANI. 10 to 50 mM PSS were enough to provide water solubility to PANI. Figure 4.5 shows that Interfacial polymerization had a lower yield than the bulk polymerization due to a less ANI monomer that were polymerized. The result shows that the higher PSS concentration, the higher PANI in aqueous phase due to the template effect but PANI yield dropped at PSS concentration higher than 20 mM because of the higher viscosity of aqueous phase which made it harder for ANI monomers to come up to polymerize on an upper phase (Detsri *et al.*, 2013).

4.2 Thin Film Assembly

4.2.1 The Effect of PSS Concentration and Polymerization Method of PANI-PSS Solution on Monolayer Deposition

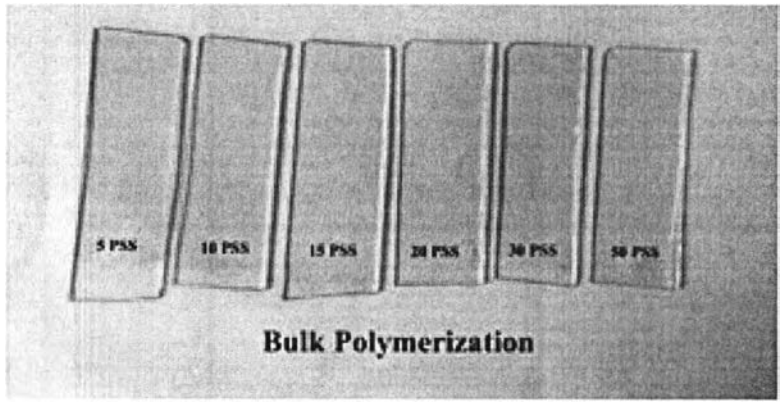

Figure 4.6 PANI monolayer film that deposited at varied PSS concentration from bulk polymerization method.

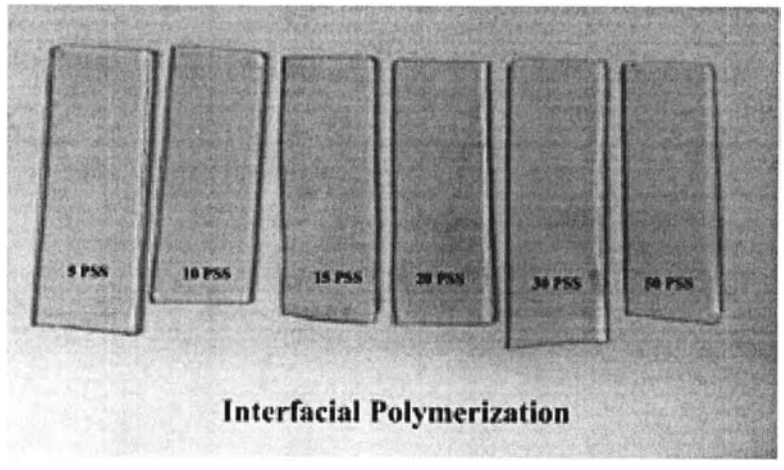

Figure 4.7 PANI monolayer film that deposited at varied PSS concentration from interfacial polymerization method.

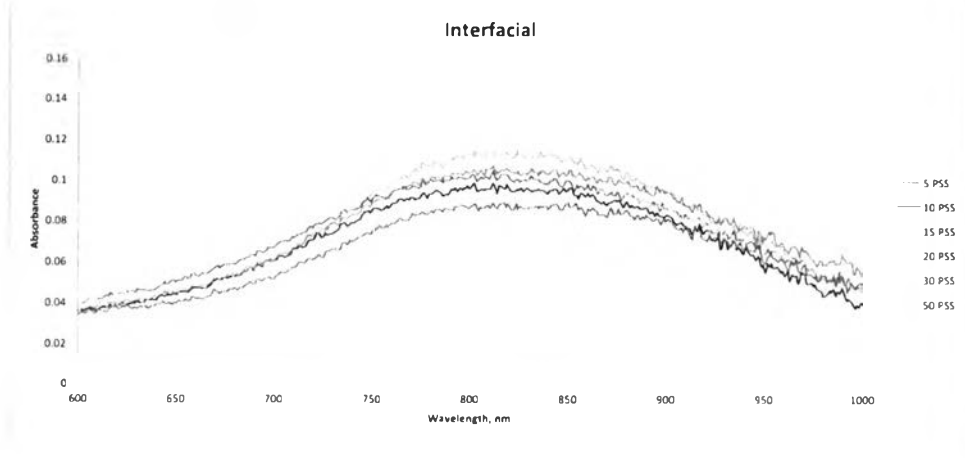

Figure 4.8 UV spectrum of monolayer of interfacial polymerized PANI-PSS on glass slide.

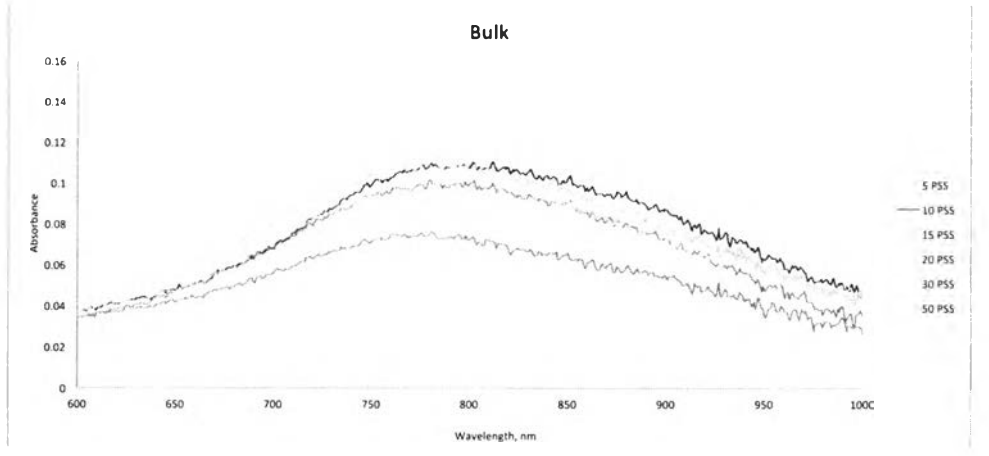

Figure 4.9 UV spectrum of monolayer of bulk polymerized PANI-PSS on glass slide.

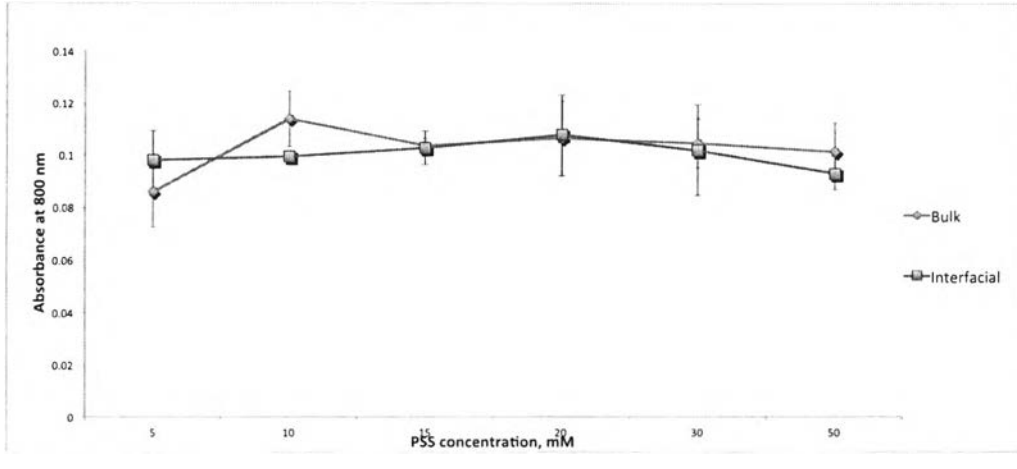

Figure 4.10 Effect of PSS concentration and polymerization method using in polymerization step on monolayer deposition.

PANI-PSS solutions were adjusted pH to 10 and the ionic strength was adjusted to 2 M NaCl. Then immersed glass slides in each solution to deposit monolayer of PANI-PSS and PANI monolayer films are shown on Figure 4.6 and Figure 4.7. The effect of PSS concentrations and the polymerization methods of PANI-PSS solution on the monolayer deposition on glass slide was studied by using

UV-Vis spectrophotometer as shown on Figure 4.8 and Figure 4.9. From Figure 4.10, UV-vis spectrum shows that the interfacial and bulk polymerization had no significant effect on the film deposition so it would be better to chose interfacial polymerization for a further research because of an ability to separate monomers out of the reaction gave a better control of the PANI polymerization. From 5 to 20 mM PSS in interfacial polymerization method, PANI was deposited on the glass slide better at higher PSS concentration because the more PSS resulted in the more PANI in the solution that could be deposit on a glass slide but at PSS concentration higher than 20 mM. PANI was deposited less on the glass slide due to the excess of PSS that competed with PANI-PSS and less PANI in the solution which already discussed on PANI synthesis part (Detsri *et al.*, 2013).

4.2.2 The Effect of pH of PANI-PSS Solution on Monolayer Deposition

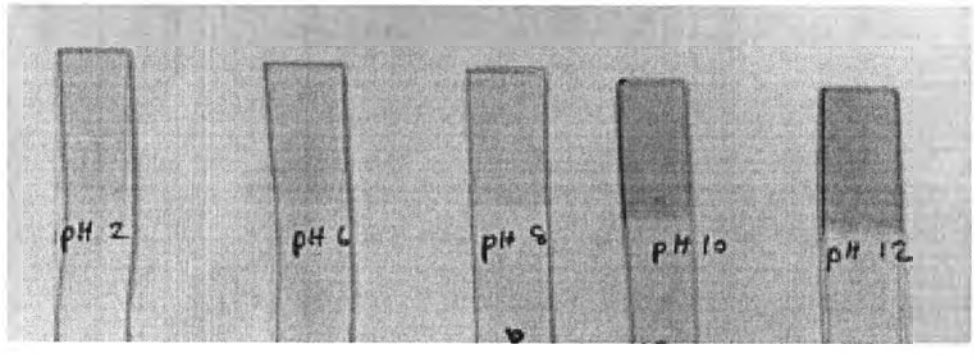

Figure 4.11 Monolayer of interfacial polymerized PANI-PSS on glass slide that deposited at different pH.

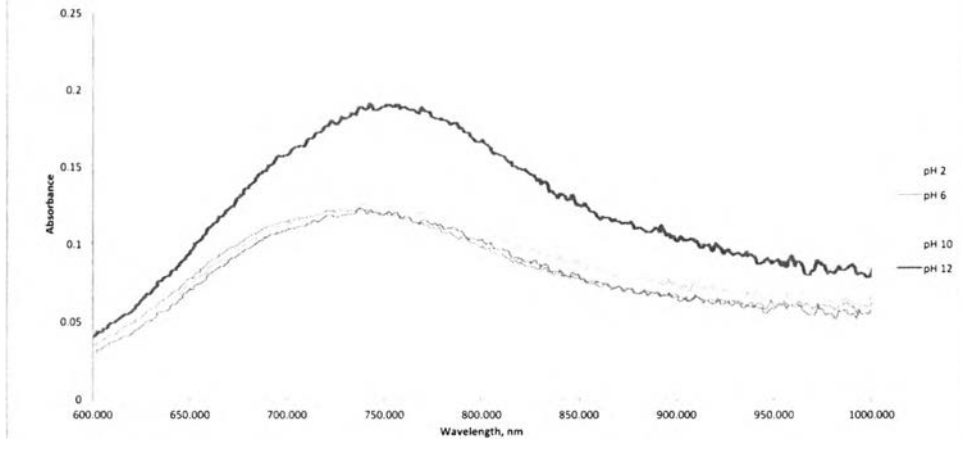

Figure 4.12 UV spectrum of monolayer of interfacial polymerized PANI-PSS on glass slide that deposited at different pH.

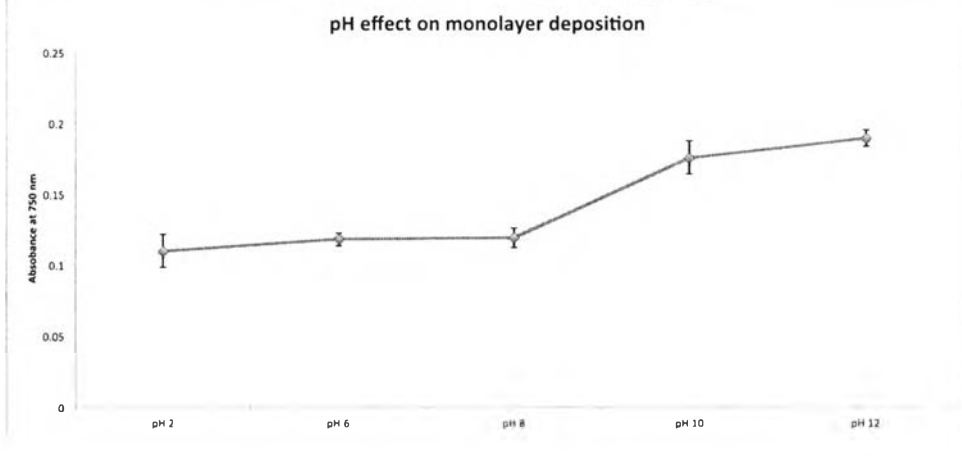

Figure 4.13 Effect of pH in PANI-PSS solution on monolayer deposition.

From the previous study, we chose PANI that synthesized by using 20 mM PSS to study the effect of pH on the deposition ability of PANI-PSS on glass slide by using UV-vis spectroscopy as shown on Figure 4.11 and Figure 4.12. Figure 4.13 shows that the deposition ability increased with higher pH because of the completed ionization.

4.3 Single Silver Loading

4.3.1 Effect of $NaBH_4$ Immersion Time on PANI-PSS/PDADMAC Multilayer Film

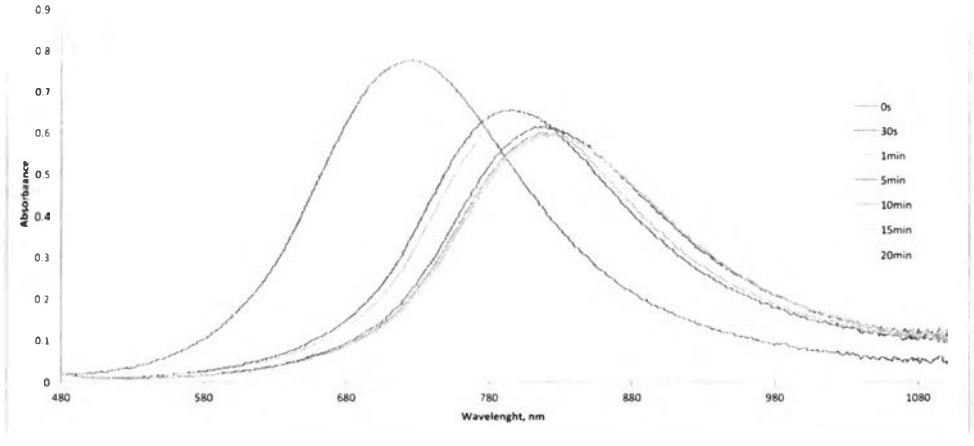

Figure 4.14 Effect of $NaBH_4$ immersion time on 11 layers of PANI-PSS/ PDADMAC multilayer film. The film was immersed in pH 2 buffer solution.

Figure 4.14 shows a red shift after dipping the PANI-PSS/ PDADMAC multilayer film into $NaBH_4$ solution. It indicated that PANI on the film probably change molecular structure by changing from quinoid unit in PANI chain to benzenoid by using $NaBH_4$ as a reducing agent and PANI were fully reduced at 5 min (Yufeng *et al.*, 2006). The result can be further confirmed by FTIR.

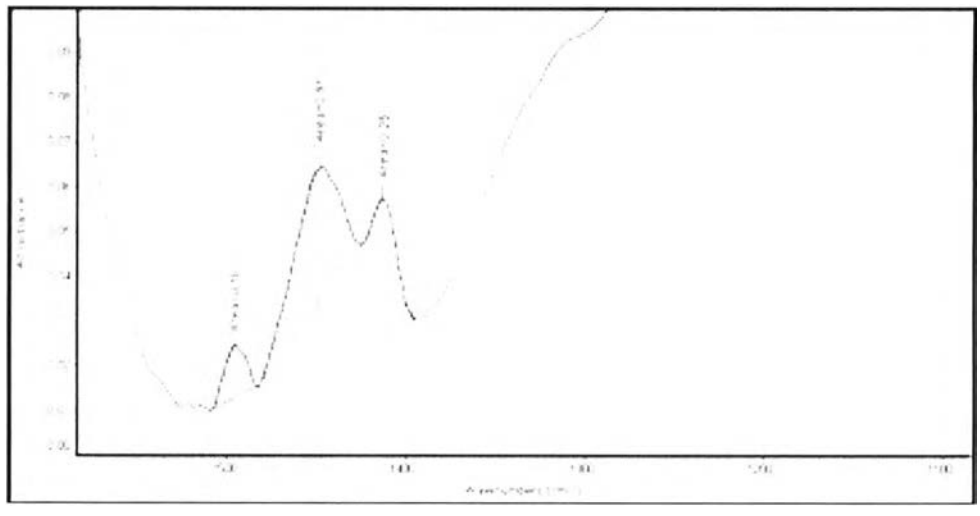

Figure 4.15 FTIR spectra of PANI using ATR mode.

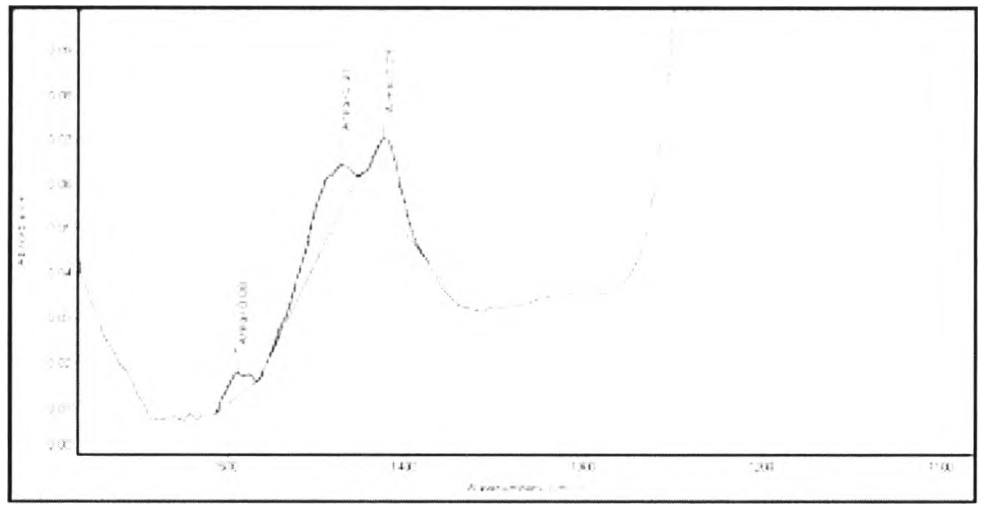

Figure 4.16 FTIR spectra of PANI/NaBH4 using ATR mode.

Table 4.1 The ratio of absorption area of quinoid to benzenoid ring

	$A_{1494\ (quinoid)}$	$A_{1410\ (benzenoid)}$
PANI	0.18	0.25
PANI/NaBH4	0.08	0.29

Figure 4.15 and Figure 4.16 show benzenoid and quinoid ring vibration at 1410 cm^{-1} and 1494 cm^{-1}, respectively. Table 4.1 indicates that PANI before reducing with $NaBH_4$ had more quinoid unit () and less benzenoid unit () than reduced PANI with $NaBH_4$ which supported the red shift of UV-vis spectrum in Figure 4.12 (Yufeng *et al.*, 2006).

4.3.2 Effect of Silver Nanoparticle in PANI-PSS/PDADMAC Multilayer Film on UV Spectrum

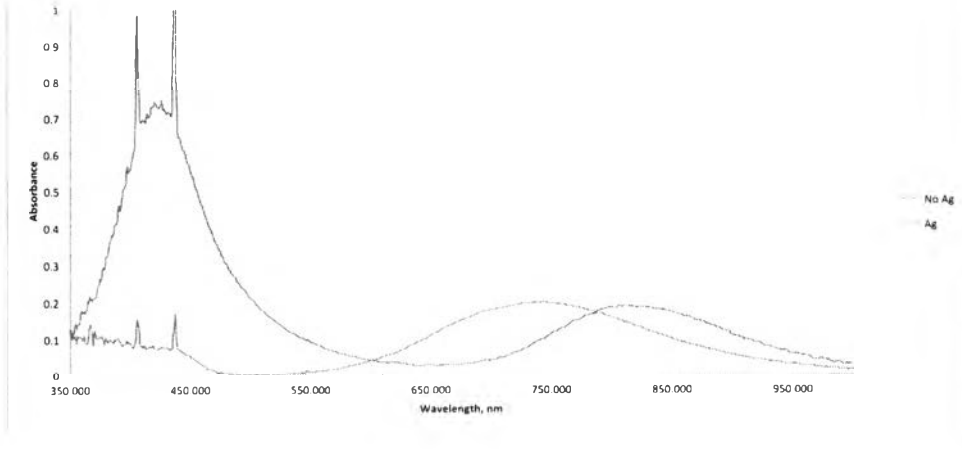

Figure 4.17 UV spectrum of original PANI-PSS/PDADMAC multilayer film, PANI-PSS/PDADMAC multilayer film with silver nanoparticles immersed in pH 2 buffer solution.

Figure 4.17 shows the UV spectrum of the film after in situ synthesis of silver nanoparticles in PANI-PSS/PDADMAC multilayer film. A red shift in PANI absorbance band from 750 nm to 810 nm and the intensity of silver plasmon band at 420 nm was increased from 0.08 to 0.75 comparing to original PANI-PSS/ PDADMAC multilayer film.

4.3.3 Effect of PANI-PSS and PDADMAC on Top on Amount of Silver After Silver Reduction

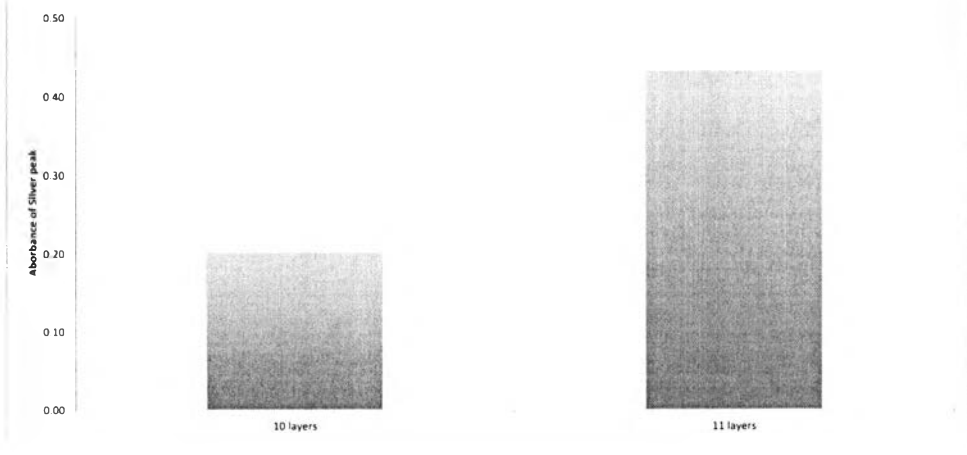

Figure 4.18 Effect of PANI-PSS and PDADMAC on top on amount of silver particle after silver reduction in 10 and 11 layers of PANI-PSS/PDADMAC multilayer film.

From Figure 4.18, PANI-PSS on the top layer promoted an absorption of Ag^+ ion into the film through an electrostatic interaction between positive charge on Ag^+ and negative charges of PANI-PSS on the film surface. On the other hand, PDADMAC on the top layer which had positive charges retarded an absorption of Ag^+ ion into the film due to the electrostatic repulsion.

4.3.4 PANI-PSS/PDADMAC and PANI-PSS/PDADMAC with In Situ Silver Nanoparticle Film Characterization

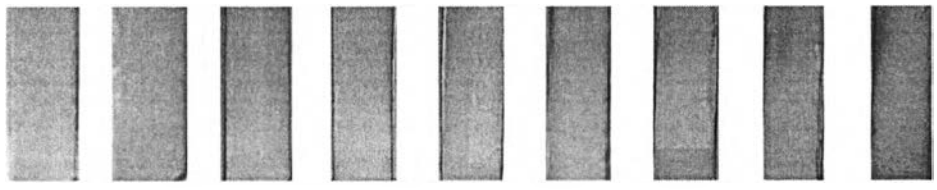

pH 2 pH 6 pH 7 pH 8 pH 9 pH 10 pH 11 pH 12 pH 14

Figure 4.19 Film color of PANI-PSS/PDADMAC multilayer film after immersed in varied pH buffer solution.

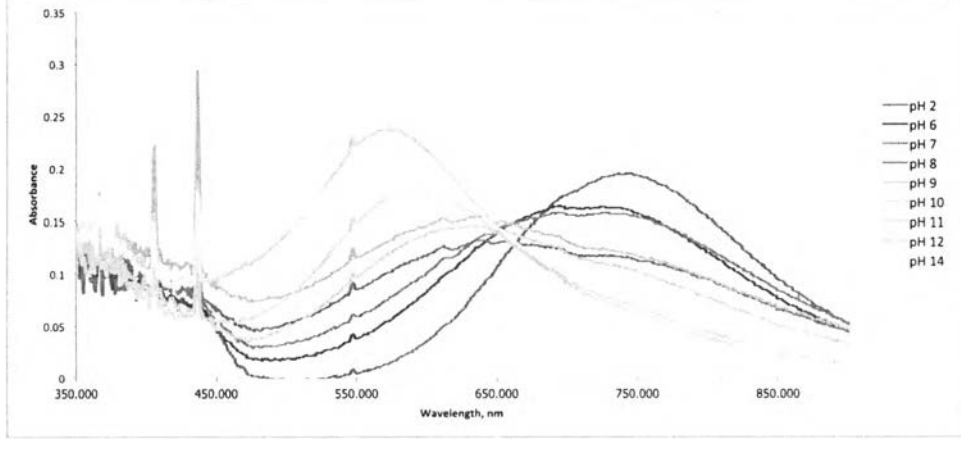

Figure 4.20 UV spectrum of PANI-PSS/PDADMAC multilayer film after immersed in varied pH buffer solution.

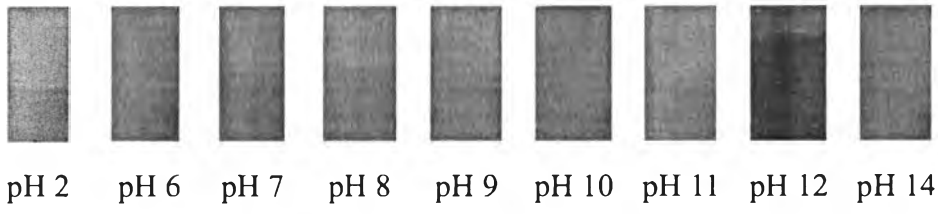

Figure 4.21 Film color of PANI-PSS/PDADMAC with in situ silver nanoparticles multilayer film after immersed in varied pH buffer solution.

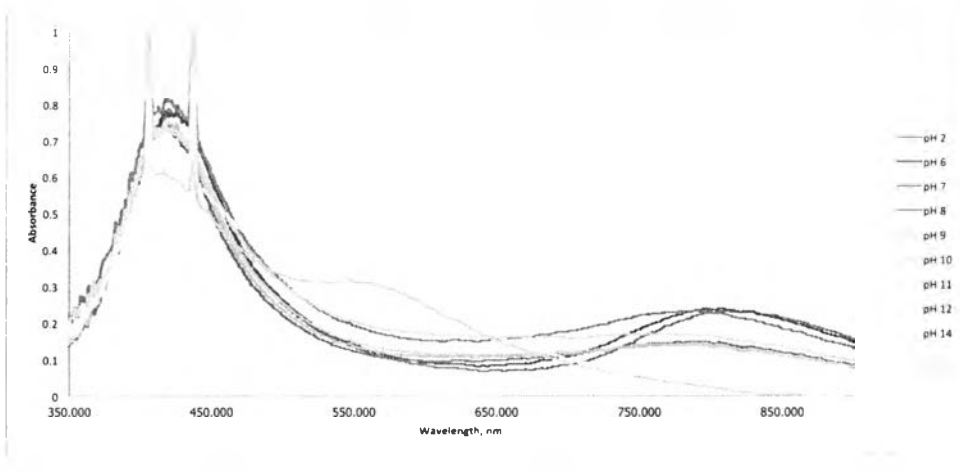

Figure 4.22 UV spectrum of PANI-PSS/PDADMAC with in situ silver nanoparticle multilayer film after immersed in varied pH buffer solution.

For PANI-PSS/PDADMAC multilayer films on Figure 4.19 and Figure 4.20, the color of the film changed from green to blue to purple when exposed to higher pH buffer solutions. For PANI-PSS/PDADMAC with in situ silver nanoparticle multilayer film in Figure 4.21, the film displayed an absorbance at 420 nm which is a character of silver nanoparticles as seen in Figure 4.22 and the color of the film changed from yellow-green to brown-green when the film exposed to higher pH buffer solution indicated that a pH sensing property of PANI still worked even with silver nanoparticles.

4.3.5 Surface Morphology

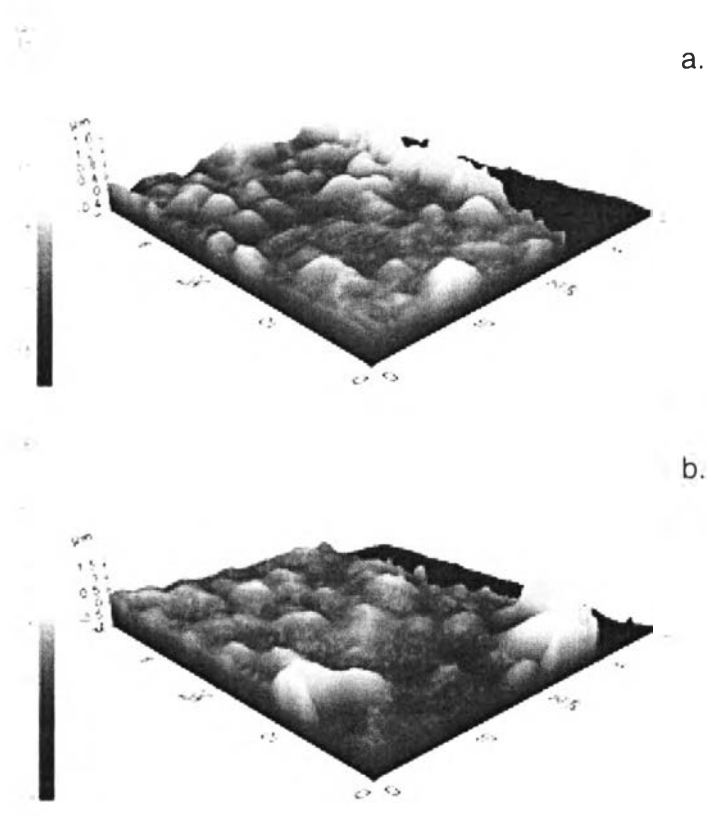

Figure 4.23 Atomic force microscope topographical scan of (a.) PANI-PSS/ PDADMAC multilayer film and (b.) PANI-PSS/PDADMAC multilayer film with silver nanoparticles.

The surface roughness was measured by an AFM as seen in Figure 4.23. The surface of the PANI film was a little rougher than PANI/Ag film due to the silver particles that were formed and filled in the gap on the film surface that could be induced to the higher conductivity.

4.3.6 Conductivity

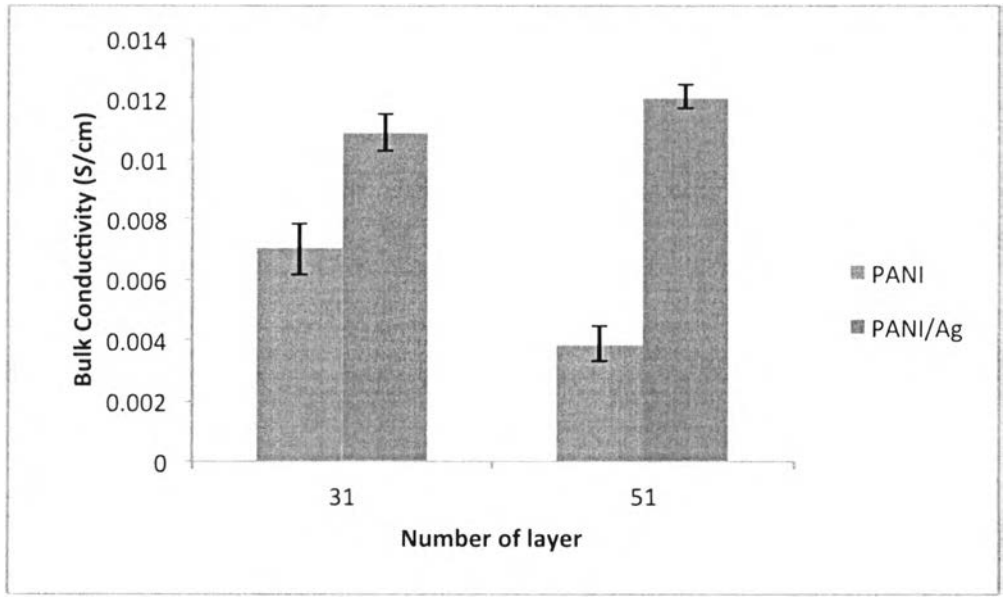

Figure 4.24 Conductivity of PANI-PSS/PDADMAC multilayer film with and without in situ silver nanoparticles.

The bulk conductivity was measured by four point probe. Figure 4.24 shows that at higher number of PANI-PSS/PDADMAC layers, the bulk conductivity tended to decrease because there was more PDADMAC layers, a non conducting polymer, which acted as an insulator wall between 2 layers of PANI-PSS. For both 31 and 51 layers film, the conductivity increased from 0.007 to 0.011 S/cm and 0.004 to 0.012 S/cm, respectively after a reduction of silver ions to silver particles.

Table 4.2 The bulk conductivity of 31 and 51 layers of PANI-PSS/PDADMAC multilayer film at before and after silver reduction

Bulk Conductivity (S/cm)				
Number of layers	31		51	
	No Ag	Ag	No Ag	Ag
Avg	0.007	0.011	0.004	0.012
% increased	55.26%		211.57%	

For 51 layers film, a percentage different between an original film and a film after silver reduction was more than 31 layers film because a thicker thickness of the film induced more silver ion to go inside the film as shown in Table 4.2.

4.4 Multi Silver Loading

4.4.1 Surface Appearance

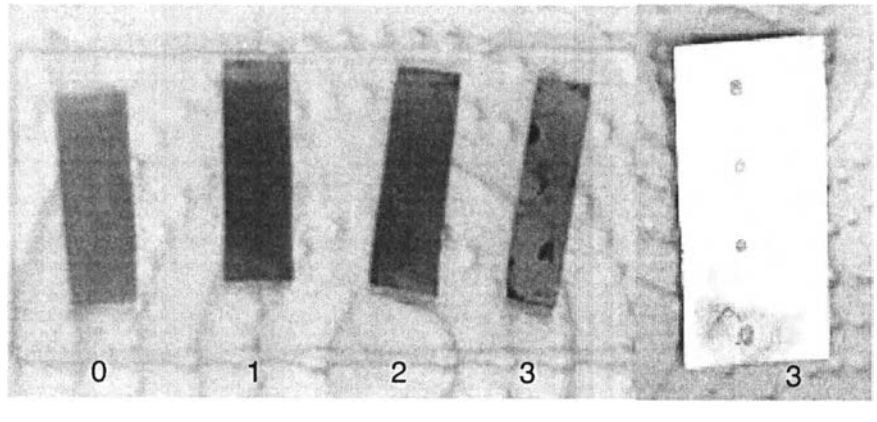

Figure 4.25 PANI-PSS/PDADMAC multilayer film after each silver reduction cycle.

Figure 4.25 shows the surface appearance of the PANI film before and after each cycle of silver reduction. Pure PANI film was green after each cycle of silver reduction, the film became more metallic and more shiny because of the formation of silver particles in the film (Anandhakumar *et al.*, 2013).

4.4.2 Surface Morphology

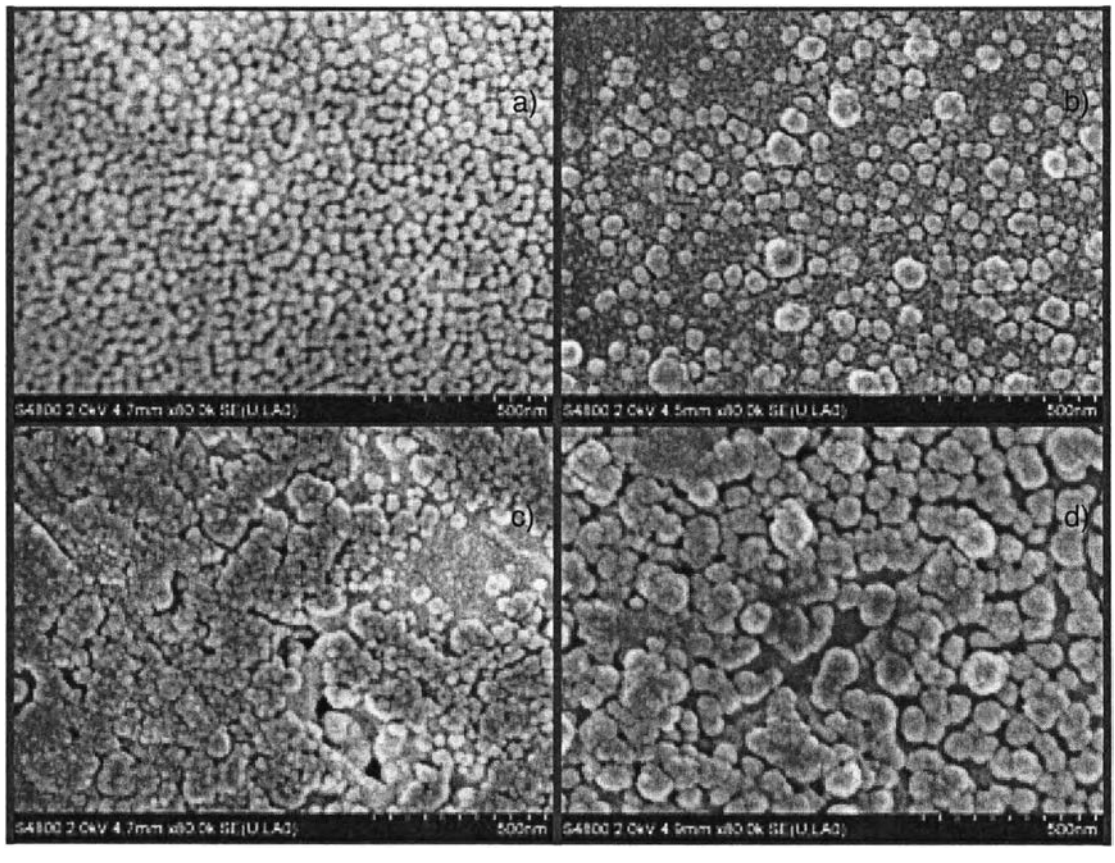

Figure 4.26 FE-SEM images of a) Original PANI-PSS/PDADMAC multilayer film, b) PANI-PSS/PDADMAC multilayer film after first cycle of silver reduction. c) PANI-PSS/PDADMAC multilayer film after second cycle of silver reduction. d) PANI-PSS/PDADMAC multilayer film after third cycle of silver reduction.

FE-SEM was used to characterize the surface morphology of the film. From Figure 4.26 a) and b) shows a granule form of PANI that was placed on the film homogeneously and (b) after first silver reduction, there were a few big particles on the the film surface which was a nucleation step following by a nucleation growth step as shown in Figure 4.26 b) and c), which was an aggregation of nuclei resulted in bigger particles.

4.4.3 Conductivity

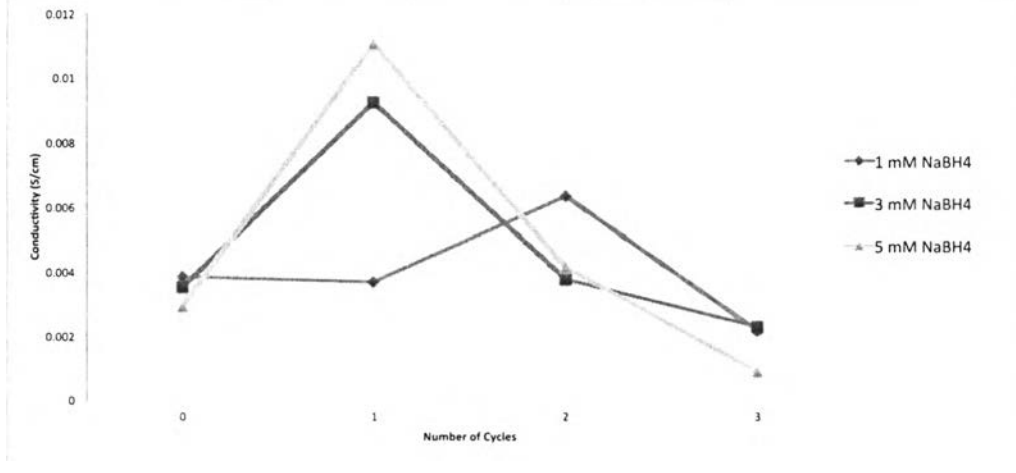

Figure 4.27 Change in conductivity of PANI-PSS/PDADMAC multilayer film as a function of number of silver reduction cycles.

The conductivity of the films was measured with a 4 point probe. Figure 4.27 shows a relationship between conductivity of the film and number of cycle with a different concentration of $NaBH_4$. 1 cycle consist of 2 steps, first is dipping a film in $AgNO_3$ and second is dipping a film in $NaBH_4$.

The conductivity of the film that was reduced with 1 mM $NaBH_4$ for the silver reduction showed a slower silver reduction rate. The conductivity of the film increased at second cycle from 0.0038 S/cm to 0.0063 S/cm due to the reduction of silver that created a conductive path in the films after a third cycle the

conductivity of the film dropped because of 2 reasons. First, the PANI film, emeraldine base, was reduced by $NaBH_4$ to leucoemeraldine which was a lower conductivity form of PANI (Yufeng *et al.*, 2006). Second reason was the PANI film, emeraldine base, was oxidized by $AgNO_3$ to pernigraniline oxidation state which also was a lower conductivity form of PANI (Stejskal *et al.*, 2009). For the film that was reduced with 3 and 5 mM $NaBH_4$, The conductivity of the film increased form 0.0035 to 0.0092 S/cm and 0.0029 to 0.011 S/cm after the first cycle, respectively. The conductivity increased because of the reduction of silver ion to silver atom and the conductivity decreased from second cycle as same as in film that was reduced with 1 mM $NaBH_4$.

In order to confirm that the conductivity decreased because of $AgNO_3$ and $NaBH_4$, The PANI films were immersed several times in $AgNO_3$ and $NaBH_4$ separately.

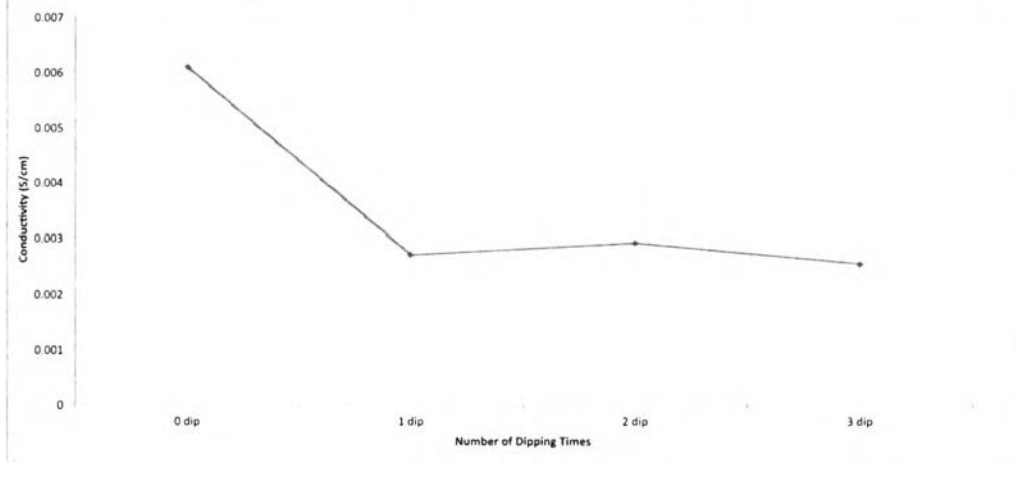

Figure 4.28 Change in conductivity of PANI-PSS/PDADMAC multilayer film as a function of number of dipping times in $AgNO_3$.

Figure 4.28 shows a relationship between conductivity of the film and number of dipping times in $AgNO_3$ solution. The conductivity of the film decreased immediately after first dipping from 0.0061 S/cm to 0.0025 S/cm due to the

oxidation of emeraldine base to pernigraniline resulted in a lower conductivity (Stejskal *et al.*, 2009).

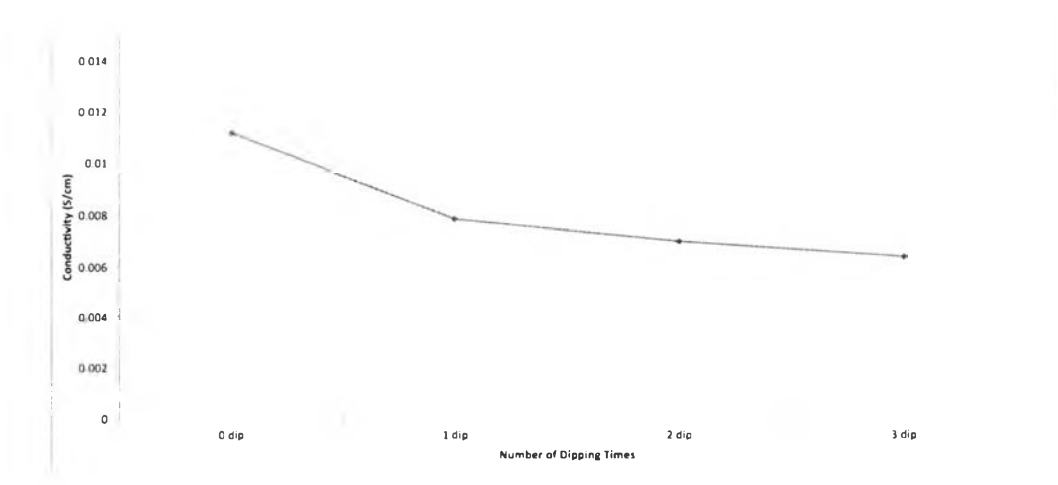

Figure 4.29 Change in conductivity of PANI-PSS/PDADMAC multilayer film as a function of number of dipping times in $NaBH_4$.

Figure 4.29 shows a relationship between conductivity of the film and number of dipping times in $NaBH_4$ solution. The conductivity of the film also decreased immediately after first dipping from 0.011 S/cm to 0.006 S/cm due to the reduction of emeraldine base to leucoemeraldine resulted in a lower conductivity (Yufeng *et al.*, 2006).

4.4.4 XRD

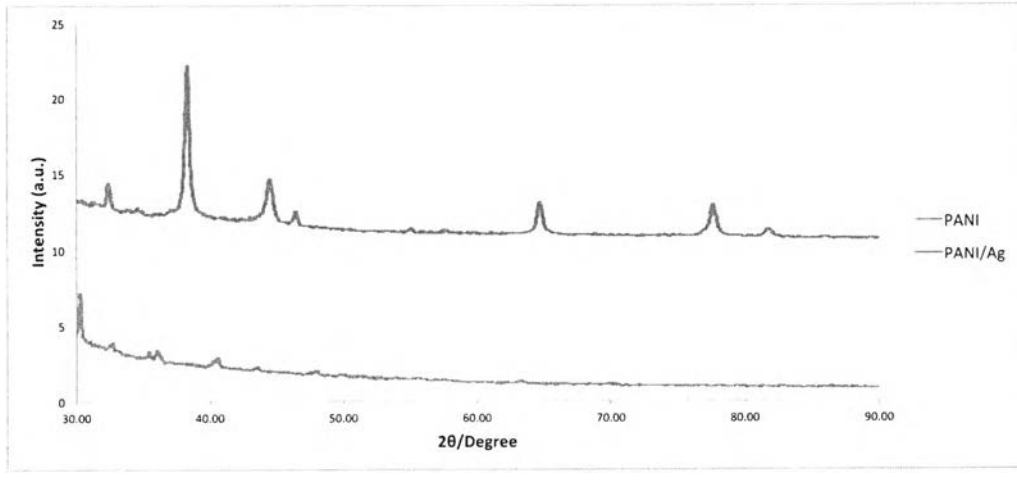

Figure 4.30 X-ray diffraction patterns of PANI-PSS/PDADMAC and PANI-PSS/ PDADMAC/Silver multilayer films.

The X-ray diffraction patterns were taken with 2°/min scanning speed from 30°-90° as shows on Figure 4.30 indicates the silver diffraction peaks at 2Θ = 38, 45, 65 and 77 which are assigned to (111) (200) (220) (311) planes of face center cubic lattice phase that correspond to Bragg's reflection.